

Spontaneous singularity formation in converging cylindrical shock waves

W. Mostert

*Mechanical and Aerospace Engineering, Princeton University, Princeton, New Jersey 08544, USA
and Graduate Aerospace Laboratories, California Institute of Technology, Pasadena, California 91125, USA*

D. I. Pullin

Graduate Aerospace Laboratories, California Institute of Technology, Pasadena, California 91125, USA

R. Samtaney

*Mechanical Engineering, Physical Science and Engineering Division,
King Abdullah University of Science and Technology, Thuwal 23955-6900, Saudi Arabia*

V. Wheatley

School of Mechanical and Mining Engineering, University of Queensland, QLD 4072, Australia



(Received 28 March 2018; published 23 July 2018)

We develop a nonlinear, Fourier-based analysis of the evolution of a perturbed, converging cylindrical strong shock using the approximate method of geometrical shock dynamics (GSD). This predicts that a singularity in the shock-shape geometry, corresponding to a change in Fourier-coefficient decay from exponential to algebraic, is guaranteed to form prior to the time of shock impact at the origin, for arbitrarily small, finite initial perturbation amplitude. Specifically for an azimuthally periodic Mach-number perturbation on an initially circular shock with integer mode number q and amplitude proportional to $\epsilon \ll 1$, a singularity in the shock geometry forms at a mean shock radius $R_{u,c} \sim (q^2\epsilon)^{-1/b_1}$, where $b_1(\gamma) < 0$ is a derived constant and γ the ratio of specific heats. This requires $q^2\epsilon \ll 1$, $q \gg 1$. The constant of proportionality is obtained as a function of γ and is independent of the initial shock Mach number M_0 . Singularity formation corresponds to the transition from a smooth perturbation to a faceted polygonal form. Results are qualitatively verified by a numerical GSD comparison.

DOI: [10.1103/PhysRevFluids.3.071401](https://doi.org/10.1103/PhysRevFluids.3.071401)

I. INTRODUCTION

Cylindrical and spherical converging shock waves, which feature prominently in contexts such as inertial confinement fusion (ICF) [1] and other settings, are known to be linearly unstable to small perturbations in their geometry [2–5]. Resultant amplitude growth generally signals a nonlinear transition from a smooth to a faceted polygonal shock profile [6–9] corresponding to triple-point formation which can break flow symmetry, an important attribute in ICF-type implosions [1]. Using the geometrical shock dynamics (GSD) description of shock evolution, we show that a singularity on the shock profile is guaranteed to form prior to cylindrical shock impact for an arbitrarily small initial perturbation. That is, in the competition between shock convergence and nonlinear shock instability, the latter always prevails. This occurs under rather general conditions assuming small perturbations on strong shocks.

Spontaneous triple-point formation also occurs in planar shocks [10–12] and detonation waves [13]. Analysis using GSD indicates that this is associated with the development of a singularity [14] characterized by loss of analyticity in the shock geometry as determined via a Fourier treatment.

This appears at a time inversely proportional to the amplitude of the initial smooth perturbation. We proceed with the analysis along these lines.

II. GEOMETRICAL SHOCK DYNAMICS FOR STRONG CYLINDRICAL SHOCKS

The kinematic equation for a moving surface described by a scalar complex variable $Z(\beta, t) = X(\beta, t) + iY(\beta, t)$ is given by [2]

$$\frac{\partial Z(\beta, t)}{\partial t} = a_0 M(\beta, t) \tilde{n}(\beta, t), \quad (1)$$

where M is the local Mach number in the interpretation of the surface as a shock wave, a_0 is the undisturbed sound speed ahead of the shock, \tilde{n} is the local normal unit vector, and β is a parameter along the shock profile. To close (1) requires an area-Mach-number rule. Given the Guderley solution, which shows monotonic and unbounded Mach-number growth for the unperturbed, collapsing shock, we make use of the strong-shock limit. It is sufficient presently that perturbations on the shock are small when the shock becomes sufficiently strong. The strong-shock area-Mach-number closure can be written as

$$M = M_0 (DZ^* DZ)^{-1/(2n)}, \quad n = 1 + \frac{2}{\gamma} + \sqrt{\frac{2\gamma}{\gamma - 1}}, \quad (2)$$

relating M to the local shock geometry where $D \equiv \partial/\partial\beta$, “*” denotes complex conjugation, γ the gas specific heat ratio, and M_0 is an initial Mach number. Curve theory yields $-i\tilde{n} = DZ/(DZ^* DZ)^{1/2}$, which completes (1). It is convenient to use the transformation $\tau = a_0 M_0 t$ to remove constants.

In GSD, the trajectory of an unperturbed cylindrical shock is given by the radius $R_u(\tau) = [-\tau(n+1)/n]^{n/(n+1)}$ with the initial shock radius (length scale) $R_u(-\tau_{\text{col}}) = 1$, where $\tau_{\text{col}} = n/(n+1)$ is a collapse time for the unperturbed shock and $R_u \rightarrow 0$, as $\tau \rightarrow 0$. In a complex GSD formulation, this corresponds to $Z_u(\beta, \tau) = R_u(\tau) e^{iq\beta}$, where $\beta \in [0, 2\pi/q)$ is periodic over an angular wedge of the cylinder with wave number q . A perturbed shock solution can be written $Z = Z_u z$, where $z(\beta, \tau) = [1 + r(\beta, \tau)] e^{i\theta(\beta, \tau)}$. Here, $r(\beta, \tau)$ corresponds to a radial perturbation of the shock, and the exponential to an azimuthal “ray-tube” perturbation; these also yield a Mach-number perturbation on the shock. Making the substitution $z = w + 1$ and after some algebra on (1), we obtain an evolution equation for the perturbation,

$$1 + w - \frac{\partial w}{\partial T} = (1 + w - iDw)[(1 + w - iDw)(1 + w^* + iDw^*)]^{-\frac{n+1}{2n}}, \quad (3)$$

$$T = \tau_{\text{col}} \ln \left(-\frac{\tau_{\text{col}}}{\tau} \right). \quad (4)$$

Here, $w = 0$ is the unperturbed solution while T maps $\tau \in [-\tau_{\text{col}}, 0)$ onto $[0, \infty)$. We aim to determine a time T at which $w(\beta, T)$ ceases to be analytic, given an analytic initial condition. This corresponds with the first time at which its Fourier coefficients \hat{w}_m fail to decay at an exponential rate with respect to the mode number m . To make (3) tractable, we replace the factor to a fractional exponent with a binomial series expansion,

$$[(1 + w - iDw)(1 + w^* + iDw^*)]^{-\frac{n+1}{2n}} = 1 + P(\beta, T), \quad (5)$$

$$P(\beta, T) = \sum_{k=1}^{\infty} b_k \{w + w^* + i(D(w^* - w)) + (w - iDw)(w^* + iDw^*)\}^k, \quad (6)$$

$$b_k = \binom{-\frac{n+1}{2n}}{k}. \quad (7)$$

This leads to

$$1 + w - \frac{\partial w}{\partial T} = (1 + P)(1 + w - iDw), \quad (8)$$

where we suppress the (β, T) dependence for clarity. This is the partial differential equation governing the evolution of the perturbation on the cylindrical shock.

III. FOURIER ANALYSIS

With

$$w(\beta, T) = \sum_{m=-\infty}^{\infty} \hat{w}_m(T) e^{imq\beta}, \quad (9)$$

an analytic initial condition will remain so for as long as the $\hat{w}_m(T)$ decay exponentially fast as $m \rightarrow \infty$. With (9), the nonlinear terms in (8), especially those embedded in P , feature repeated Cauchy products of the series (9) of successively higher orders according to the exponent k in (6), so that the Fourier representation of (8) is complicated if written out in full. Since the Fourier representation of each quantity on the right-hand side can be arranged as a coefficient appearing in $\sum_m (\dots) e^{imq\beta}$, (8) has the compact form

$$\frac{d\hat{w}_m}{dT} = i\widehat{D}w_m + i\widehat{P}Dw_m - \widehat{P}_m - \widehat{wP}_m, \quad (10)$$

so that the quantities on the right-hand side are thought of as the m th Fourier coefficients of their associated (repeatedly convolved) infinite series.

We introduce the initial condition, which will lead to a tractable form of (10), using a perturbation of large wave number $q \gg 1$ and small amplitude $O(\epsilon)$, $\epsilon \ll 1$,

$$w(\beta, 0) = e^{i\epsilon \sin q\beta} - 1, \quad \hat{w}_{\pm 1}(0) = \pm J_1(\epsilon), \quad (11)$$

and $\hat{w}_{\pm m} = O(\epsilon^{|m|})$, where J_1 is the Bessel function of the first kind with $J_1(\epsilon) = \epsilon/2 + O(\epsilon^3)$. This is equivalent to choosing $z(\beta, 0) = e^{i\theta(\beta)}$ with $\theta(\beta) = \epsilon \sin q\beta$ [and $r(\beta, 0) = 0$], corresponding with an initially circular shock with a Mach-number perturbation. Following Refs. [14,15], we assume that the order relation $\hat{w}_{\pm m} = O(\epsilon^{|m|})$ holds over the range of times of interest, and further, that the coefficients $\hat{w}_m(T)$ can be expanded in a power series,

$$\hat{w}_m(T) = \epsilon^{|m|} \sum_{l=0}^{\infty} W_{m,l}(T) \epsilon^l. \quad (12)$$

After substitution into (10), the system decomposes into a set of subsystems, each corresponding with an index l in (12). The leading-order subsystem corresponds to the leading-order coefficient of (12), $l = 0$, and in that subsystem, all the infinite Cauchy products have been truncated to finite sums. In particular, a k -fold Cauchy product $\sum_{r_1+r_2+\dots+r_k=m} (\dots)$ is truncated to operate over only the finite set of indices $r_1, \dots, r_k \geq 1$. Now, for small values of $|m|$, solutions to (10), with $W_m \equiv W_{m,0}$ substituted for \hat{w}_m , may be profitably sought.

IV. ANALYTICAL RESULTS

For $m = \pm 1$, solving the coupled system of homogeneous ordinary differential equations (ODEs) (10) produces the solution

$$W_1(T) = C^+ e^{s_1 T} + C^- e^{s_{-1} T}, \quad (13)$$

$$W_{-1}(T) = C^+ M^+ e^{s_1 T} + C^- M^- e^{s_{-1} T}, \quad (14)$$

where $s_{\pm 1} = [-b_1 \pm \sqrt{q^2(1 + 2b_1) + b_1^2}]$, and C^+ , M^+ are $O(1)$ [that is, smaller than $O(q)$] constants dependent on the initial condition. Following the simplification made earlier, this corresponds to the linear solution for the system. Equations (13) and (14) describe oscillatory growth (since $b_1 < 0$) in the first perturbed mode, immediately capturing the well-known linear instability of the shock. The growth rate $-b_1 T$ matches the result of Ref. [3] exactly in the strong-shock limit and does not depend on the wave number q . The planar shock result [14] is recovered with the time transformation $T' = qT$ in the limit $q \rightarrow \infty$.

For any $|m| > 1$, the ODE system (10) is inhomogeneous and captures nonlinear behavior which we show leads to singularity formation. In these inhomogeneous equations, the forcing term only involves the coefficients $W_{\pm l}$, where $|l| < |m|$ for a given $|m|$; hence the solution process is sequential in m . We seek the asymptotic behavior of $W_{|m|}$ for large $|m|$, since it is in this region that we can determine whether $w(\beta, T)$ is analytic. It is unfeasible to produce solutions into this region sequentially. Instead, the solutions for the first few $|m|$ informs an ansatz form for any $W_m(T)$, which is amenable to an asymptotic analysis. We derive this ansatz form as follows. For $m = 2$, the forcing term depends only on a quadratic in $W_{\pm 1}$, since our leading-order subsystem contains no cubics or other higher-order terms at $m = 2$. From (13) and (14), this will yield a solution $W_{\pm 2}$ which grows as $e^{-2b_1 T}$. Now suppose W_m grows as $e^{-mb_1 T}$. In the forcing term for W_{m+1} , each inhomogeneous contribution grows as $e^{-(m+1)b_1 T}$ since it involves k -fold products of W_{r_i} , $i = 1, \dots, k$, such that $\sum_i^k r_i = m$. Hence the assumption is justified by induction. Second, since the homogeneous solution for any m grows only as $e^{-b_1 T}$, therefore the particular integral arising from the inhomogeneous contribution dominates the homogeneous solution for large m , large T , or both. Third, crucially, although each contribution in the forcing term grows at the same rate in T , the quadratic contributions dominate for large wave numbers q (but see the further discussion in Sec. VI). This follows from the solution $m = 2$ being $O(q^2)$; a similar inductive argument to the above shows that $W_m = O(q^{2(m-1)})$ apart from the growth in time, but in this case the only contributions to the particular integral of this order come from the quadratic term. This leads to a consistent ansatz for the $W_{\pm m}$ in the limit of large q ,

$$W_m(T) = (C^\pm)^m q^{2(m-1)} \lambda_m^\pm e^{-mb_1 T \pm i\omega_m T} + O(e^{-(m-1)b_1 T}), \quad (15)$$

$$W_{-m}(T) = (C^\pm)^m M^\pm q^{2(m-1)} \lambda_m^\pm e^{-mb_1 T \pm i\omega_m T} + O(e^{-(m-1)b_1 T}), \quad (16)$$

where \pm indicates summation over $+$ and $-$. The various coefficients are given by

$$\lambda_m^\pm = \frac{K^\pm}{2(m-1)} \sum_{r_1+r_2=m} r_1 r_2 \lambda_{r_1}^\pm \lambda_{r_2}^\pm, \quad m \geq 2, \quad (17)$$

$$K^\pm = \pm \frac{(1 \mp \sqrt{1+2b_1})K_B^\pm + b_1^2[(M^\pm)^2 - 1]}{b_1 \sqrt{1+2b_1}}, \quad (18)$$

$$K_B^\pm = -b_1 + 2M^\pm b_1 - b_2 + 2M^\pm b_2 - (M^\pm)^2 b_2, \quad (19)$$

$$M^\pm = \frac{b_1}{1 \mp \sqrt{1+2b_1} + b_1}, \quad (20)$$

$$C^\pm = \frac{-(1+2b_1) \pm \sqrt{1+2b_1}}{4\sqrt{1+2b_1}}, \quad (21)$$

and $\lambda_1^\pm = 1$.

The asymptotic behavior of (15) and (16) depends on the associated asymptotic form of the recursion relation (17). This final derivation follows Moore [15], also used in Ref. [14]. First, a

generating function is written for the λ_m , satisfying an ODE consistent with (17),

$$g(x) = \sum_{m=1}^{\infty} |\lambda_m| x^m, \quad \frac{d}{dx} \left(\frac{g(x)}{x} \right) = \frac{|K|}{2} \left(\frac{dg}{dx} \right)^2, \quad (22)$$

defined on the complex x plane with the initial condition $g(0) = 1$, where $|K| = |K^\pm|$, and which has the solution

$$g(x) = -\frac{2W(-x|K|) + W^2(-x|K|)}{2|K|}, \quad (23)$$

where W is the Lambert W -function principal branch. $g(x)$ has a singularity at $x_c = -(|K| e)^{-1}$ on the real line. By Darboux's method [16], the dominant asymptotic behavior of $g(x)$ near x_c can be compared asymptotically to a known function $h(x)$ if $h(x)$ is analytic in some disk around x_c , $h(x) - g(x)$ is continuous in this disk, and the Laurent series expansion coefficients of $h(x)$ have a known asymptotic behavior. A suitable candidate is

$$h(x) = \frac{2\sqrt{2}(1 - ex|K|)^{3/2}}{3|K|} = \sum_{m=0}^{\infty} a_m x^m, \quad (24)$$

whose power-series coefficients a_m behave asymptotically according to the binomial theorem,

$$a_m \simeq \frac{1}{2\pi} |K|^{m+1} e^m m^{-5/2} \sim |\lambda_m|, \quad (25)$$

where the final asymptote relation is the result of Darboux's method. Substituting (25) into (15) yields the asymptotic result,

$$W_m(T) = \frac{|C^\pm|^m q^{2(m-1)}}{\sqrt{2\pi}} |K|^{m+1} e^m m^{-5/2} e^{-mb_1 T \pm i\omega_m T + iQ^\pm}, \quad (26)$$

and similarly for $W_{-m}(T)$ in (16), where $Q^\pm = \arg[(K^\pm C^\pm)^m \lambda_m^\pm]$. Since $w_m = W_m \epsilon^{|m|} + \text{HOT}$, this implies the Fourier coefficients of the perturbation w decay exponentially with m for as long as

$$m[\log(e|C^\pm K^\pm| q^2 \epsilon) - b_1 T] < 0, \quad m \gg 1, \quad (27)$$

during which time w remains analytic. This analyticity is lost at the critical stretched time T_c , corresponding with singularity formation, when

$$T_c = \frac{1}{b_1} \log(e|C^\pm K^\pm| q^2 \epsilon). \quad (28)$$

The stretched time T can be interpreted as the radius of an equivalent unperturbed shock $R_u = e^{-T}$, hence equivalently the *critical shock radius* is

$$R_{u,c} = (e|C^\pm K^\pm| q^2 \epsilon)^{-1/b_1}. \quad (29)$$

Finally, (28) can also be written in terms of the critical *elapsed time* $\tilde{\tau}_c$, measured from the initial condition using (4),

$$\frac{\tilde{\tau}_c}{\tau_{\text{col}}} = (1 - [e|C^\pm K^\pm| q^2 \epsilon]^2), \quad \tau_{\text{col}} > 0, \quad (30)$$

with $\tilde{\tau} = \tau + \tau_{\text{col}}$, recalling that $\tau < 0$ is the ‘‘shock time’’ and the point of collapse corresponds with $\tau = 0$. Thus, $\tilde{\tau} \rightarrow \tau_{\text{col}}$ as the shock nears collapse, and the left-hand side of (30) approaches unity as $\epsilon \rightarrow 0$. Equations (28)–(30) are our primary result. Their implications are that, first, a singularity in the shock geometry is guaranteed to form prior to shock impact at the axis, for arbitrarily small ϵ . This follows from $\epsilon > 0$, guaranteeing that the left-hand side of (30) is smaller than unity, or, equivalently, that T_c is finite in (28) or $R_{u,c}$ is positive in (29). Second, the dimensionless radius at

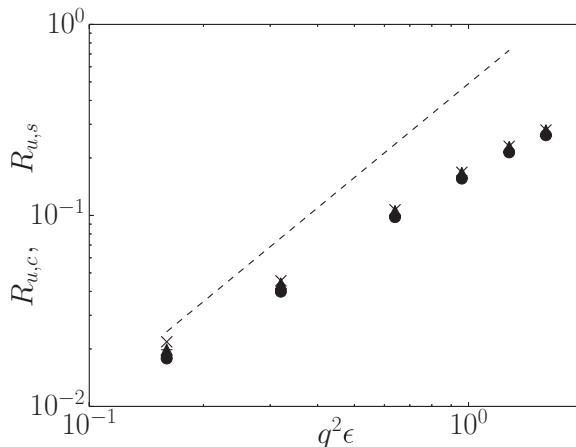


FIG. 1. Critical shock radius against wave-number perturbation $q^2\epsilon$. +: $M_0 = 20$, $q = 16$; ●: $M_0 = 10$, $q = 16$; ×: $M_0 = 20$, $q = 8$; ▲: $M_0 = 10$, $q = 8$. The dashed line shows (29) for $q = 16$ with power-law exponent $-1/b_1 \simeq 1.632$. Numerical data show an exponent of approximately 1.15.

which the singularity forms is independent of the initial choice of M_0 , which was scaled out of the problem by definition of τ . This is a direct consequence of our use of the strong-shock approximation (2) and may not hold for general initial M_0 . Third, we expect the result to be more accurate at large times T_c , or, equivalently, in the (distinguished) limit $q^2\epsilon \ll 1$.

V. NUMERICAL COMPARISON

We use a two-dimensional GSD code [10] based on the method of Schwendeman [17] adapted for gasdynamic shocks. The initial condition is generated in an initially purely cylindrical shock, with a Mach-number perturbation

$$M(\beta, 0) = M_0(1 + q\epsilon \cos(q\beta))^{-1/n}. \quad (31)$$

We use $q^2\epsilon = 0.16, 0.32, 0.64, 0.96, 1.28, 1.6$ with $q = 8, 16$ and $M_0 = 10, 20$. The numerics produce an unscaled time t_s for the time to shock-shock (triple-point) formation, which we convert to an equivalent radius $R_{u,s}$ for convenience of comparison. Figure 1 shows the numerical data together with (29), which features the power-law exponent $-1/b_1 \simeq 1.632$ for $\gamma = 5/3$. The associated constants are $|C^\pm| \simeq 0.277$ and $|K^\pm| \simeq 0.858$. The prediction somewhat overestimates the best-fit power-law exponent using the GSD numerical results, which is ~ 1.15 . The numerical data do show a slightly convex form with the suggestion of an asymptotic trend to the dashed line for smaller $q^2\epsilon \rightarrow 0$ that can be obtained with the present numerical method. This distinguished limit, corresponding with $R_{u,c} \rightarrow 0$, is difficult to achieve numerically since the solver becomes increasingly ill conditioned as the shock nears the origin. Nevertheless, the numerics agree with the predictions that the critical radius is insensitive to the initial Mach number M_0 , and collapses on $q^2\epsilon$. Indeed, the guaranteed formation of a singularity in the limit $\epsilon \rightarrow 0$ is suggested by the numerical results in support of the analytical conclusion.

VI. DISCUSSION AND CONCLUDING REMARKS

The present analysis reproduces the known GSD result that the growth rate, but not the oscillation frequency, of a perturbation on a cylindrical shock is independent of its wave number [3,18]. Further, the present growth rates match those found in Ref. [3], a GSD study of both cylindrical and spherical shock stability. In contrast, the rigorous but strictly linear Euler-based analysis of

Murakami *et al.* [5] for converging spherical shocks finds a cutoff wave number in the growth-rate dependence of perturbations, above which disturbances are damped. At low wave numbers, the GSD and Euler results for the linear stability of the spherical implosion are in satisfactory agreement. For the linear stability of planar shocks, GSD gives neutral stability whereas Freeman [19] shows a perturbation decay.

Yet despite damping in the linear approximation, weakly nonlinear, Euler-based analysis [11,20] and fully nonlinear shock-capturing numerical simulations of perturbed planar shocks [21] show strong evidence of kink/triple-point formation from smooth initial conditions, behavior clearly captured by GSD [10,14]. For cylindrical converging shocks, experimental holographic interferometry [7], Euler-based numerical simulations [7,8], and GSD simulations [6,9,10] all show an initial perturbation growth leading to triple-point, or with GSD, shock-shock formation. The onset of singularity and subsequent triple-point formation for these flows is driven physically by nonlinear transfer of energy from small to large wave numbers leading to a nonlinear amplitude reinforcement at arbitrarily large wave numbers. Since this cannot be obtained from a linear stability analysis, we conclude that possible linear damping at sufficiently large wave numbers, not well reproduced by GSD, is a subdominant mechanism in the nonlinear dynamics of incipient singularity formation found presently.

Our analysis requires $q^2\epsilon \rightarrow 0$, $q \gg 1$, $q^2\epsilon < 1$ for consistency. The principal result, namely, the guaranteed singularity formation preceding shock collapse, is supported by the numerical data at a qualitative level with indication of numerical agreement in the distinguished limit. As for the planar case [14], singularity formation may indeed be a precursor of triple-point formation. This suggests that any smoothly perturbed cylindrical shock is guaranteed to undergo a transition to the polygonal shock surface considered in Ref. [6]. The result may have significant implications for fusion problems featuring converging shock waves.

ACKNOWLEDGMENT

This research was supported by the KAUST Office of Sponsored Research under Award No. URF/1/2162-01.

-
- [1] J. Lindl, O. Landen, J. Edwards, E. Moses, and NIC Team, Review of the national ignition campaign 2009–2012, *Phys. Plasmas* **21**, 020501 (2014).
 - [2] G. Whitham, *Linear and Nonlinear Waves* (Wiley, Hoboken, NJ, 2011).
 - [3] J. H. Gardner, D. L. Book, and I. B. Bernstein, Stability of imploding shocks in the CCW approximation, *J. Fluid Mech.* **114**, 41 (1981).
 - [4] D. L. Book, Linearized geometrical-dynamics treatment of the stability of converging shocks, *Phys. Fluids A* **2**, 635 (1990).
 - [5] M. Murakami, J. Sanz, and Y. Iwamoto, Stability of spherical converging shock wave, *Phys. Plasmas* **22**, 072703 (2015).
 - [6] D. W. Schwendeman and G. B. Whitham, On converging shock waves, *Proc. R. Soc. London, Ser. A* **413**, 297 (1987).
 - [7] M. Watanabe and K. Takayama, Stability of converging cylindrical shock waves, *Shock Waves* **1**, 149 (1991).
 - [8] S. I. Betelu and D. G. Aronson, Focusing of Noncircular Self-Similar Shock Waves, *Phys. Rev. Lett.* **87**, 074501 (2001).
 - [9] D. W. Schwendeman, On converging shock waves of spherical and polyhedral form, *J. Fluid Mech.* **454**, 365 (2002).
 - [10] W. Mostert, D. I. Pullin, R. Samtaney, and V. Wheatley, Geometrical shock dynamics for magnetohydrodynamic fast shocks, *J. Fluid Mech.* **811**, R2 (2017).

- [11] P. Clavin, Nonlinear analysis of shock-vortex interaction: Mach stem formation, *J. Fluid Mech.* **721**, 324 (2013).
- [12] G. Lodato, L. Vervisch, and P. Clavin, Direct numerical simulation of shock wavy-wall interaction: Analysis of cellular shock structure and flow patterns, *J. Fluid Mech.* **789**, 221 (2016).
- [13] L. M. Faria, A. R. Kasimov, and R. R. Rosales, Theory of weakly nonlinear self-sustained detonations, *J. Fluid Mech.* **784**, 163 (2015).
- [14] W. Mostert, D. I. Pullin, V. Wheatley, and R. Samtaney, Singularity formation on perturbed planar shock waves, *J. Fluid Mech.* **846**, 536 (2018).
- [15] D. W. Moore, The spontaneous appearance of a singularity in the shape of an evolving vortex sheet, *Proc. R. Soc. London, Ser. A* **365**, 105 (1979).
- [16] F. W. J. Olver, *Asymptotics and Special Functions* (Academic, New York, 1974), p. 310.
- [17] D. W. Schwendeman, A new numerical method for shock wave propagation based on geometrical shock dynamics, *Proc. R. Soc. London, Ser. A* **441**, 331 (1993).
- [18] G. B. Whitham, A new approach to problems of shock dynamics Part I Two-dimensional problems, *J. Fluid Mech.* **2**, 145 (1957).
- [19] N. C. Freeman, On the stability of plane shock waves, *J. Fluid Mech.* **2**, 397 (1957).
- [20] B. Denet, L. Biamino, G. Lodato, L. Vervisch, and P. Clavin, Model equation for the dynamics of wrinkled shockwaves: Comparison with DNS and experiments, *Combust. Sci. Technol.* **187**, 296 (2015).
- [21] G. Lodato, L. Vervisch, and P. Clavin, Numerical study of smoothly perturbed shocks in the Newtonian limit, *Flow Turbulence Combust.* **99**, 887 (2017).